GEOPHYSICAL RESEARCH LETTERS, VOL. 24, NO. 23, PAGES 3081-3084, DECEMBER 1, 1997

Geometry, kinematics and rates of deformation in a normal fault segment boundary, central Greece

N.C. Morewood and G.P. Roberts

The Research School of Geological and Geophysical Sciences, Birkbeck and University College, London, U.K.

Abstract. The geometry, kinematics and rates of deformation within a fault segment boundary between the ends of two major active normal fault segments have been investigated through examination of a faulted 126 ka marine terrace. Slip-vector azimuths defined by striations on the faults indicate N-S extension on *c.* E-W faults, sub-parallel to those from earthquake focal mechanisms, together with significant and contemporaneous E-W extension on *c.* N-S faults. Summed rates of E-W extension along a *c.* 550 m transect (0.17 mm/yr) are comparable with those for N-S extension (0.20 mm/yr) along a *c.* 350 m transect. Our observations show that distributed non-plane strain extension occurs in fault segment boundaries and this should be noted when studying fault-tip fracture toughness and regional deformation rates.

Introduction

Normal fault systems consist of individual fault segments, tens of km in length, separated by areas of low fault displacement, or fault segment boundaries. With the exception of Susong *et al.* (1990) and Janecke (1993), who mapped two fault segment boundaries in the western U.S.A., few studies of fault segment boundaries exist. Moreover, very few data are available on their geometry, kinematics and rates of deformation. The Perachora Fault Segment Boundary (PFSB) is situated between the recently-ruptured Xilokastro and South Alkyonides Fault Segments (Roberts 1996) (Fig. 1) and well-exposed minor faults cut a 126 ka marine terrace. We present detailed maps of two sub-areas within the PFSB and describe the geometry, kinematics and rates of deformation. We discuss their implications for studies of fault-tip fracture toughness and regional deformation rates.

Geological background

The Gulf of Corinth study area lies in one of the fastest extending regions of the Earth's continental crust (*c.* 10 mm/yr of N-S extension, (Billiris *et al.* 1991)). The Xilokastro and South Alkyonides Fault Segments bound the southern sides of active marine depocentres. The eastern segment was ruptured at the surface in 1981 (Jackson *et al.* 1982) and the western segment may have been ruptured in 1928 and 1981 (Armijo *et al.* 1996). The coseismic throws associated with the onshore 1981 earthquake ruptures, decreased to zero towards the PFSB (Jackson *et al.* 1982). Existing fault-slip data (Roberts 1996) (Fig. 1) show a component of along-strike extension at the ends of fault segments and provoked our interest in the current study.

Method and results

Seventy eight faults have been mapped within an area *c.* 4 km by *c.* 3.5 km (Figs. 2 and 3), including c. E-W and c. N-S striking faults. Lineations on the faults, such as scratches, grooves and corrugations, were measured wherever possible. Slip is mainly dip-slip, producing both N-S and E-W extension. Uplifted 126 ka raised-beach-shoreface sediments (Vita-Finzi 1993) are downthrown by the faults. This allows us to calculate deformation rates averaged over the past 126 ka. The 126 ka sediments are not overlain by younger deposits so that the faulting must have broken the ground surface, presumably during palaeo-earthquake rupturing prior to 1981, but post-126 ka. We assume that these faults did not initiate after 126 ka; if they did, the calculated deformation rates would be higher. The 126 ka sediments are, in many places, underlain by algal bioherms. The algal bioherms are un-dated, but we assume they also formed at about 126 ka because if they were significantly older they would be displaced by greater amounts than the raised beach on faults that cut both units; however, similar displacements are observed. For each fault, mean displacement vector azimuths were calculated from our measurements of lineations.

With the above information, we used trigonometry to calculate the average deformation rates over 126 ka in the vertical plane containing the displacement vector azimuth. These include (1) the rate of throw accumulation, (2) the horizontal extension rate and (3) the displacement rate (Table 1). Averaged displacement-rates for 126 ka on individual faults range from 0.01 to 0.31 mm/year, whereas rates of horizontal extension and throw accumulation range between 0.01 and 0.14 mm/year and 0.01 and 0.28 mm/year respectively.

We have illustrated the rates of horizontal extension with vector arrows on maps (Fig. 4). The orientations of the arrows show the directions of movement and their lengths are proportional to the rates of horizontal extension averaged over the past 126 ka. Levels of certainty are indicated in Fig. 4. The deformation is clearly not plane-strain. We have summed horizontal extension rates along two sub-perpendicular transects, oriented c. N-S and c. E-W, to investigate the complex non-plane strain nature of the extension (Fig. 4). The transects cross as many faults as possible to maximise the summed extension rates. We do not think that we have missed any major faults on our transects. Trigonometry was used to calculate the components of motion parallel to the N-S and E-W transects

Paper number 97GL03100.
0094-8534/97/97GL-03100$05.00

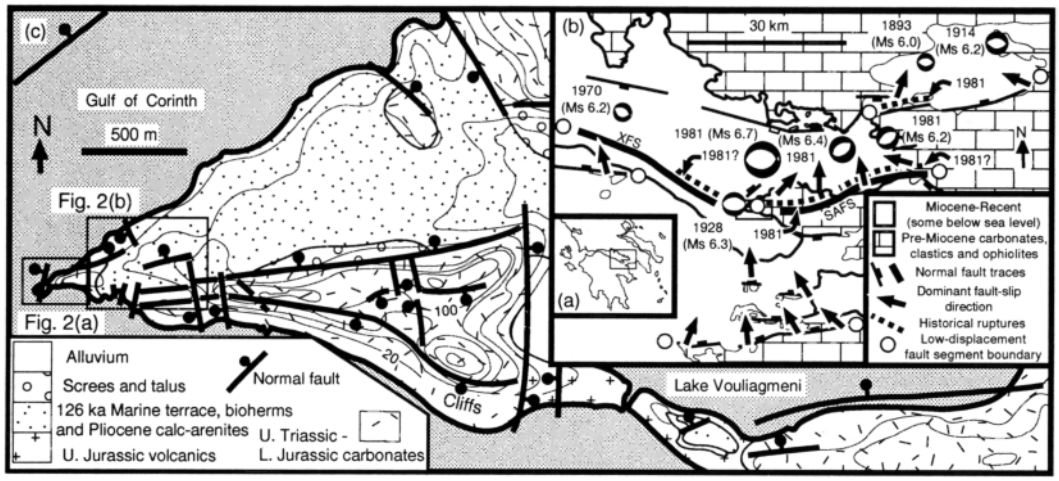

Figure 1. (a) Map of the Aegean. Inset box locates (b). (b) Thick lines show the Xilokastro (XFS) and South Alkyonides Fault Segments (SAFS). Focal mechanisms are shown for all earthquakes >Ms 6.0 in the last 104 years (from Billiris *et al.* 1991). Known and suspected surface ruptures are from Jackson *et al.* (1982), Abercrombie *et al.* (1995), and Hubert *et al.* (1996). Dominant fault-slip directions from Roberts (1996). Inset box locates (c). (c) Geological map of the Perachora Peninsula. Inset boxes locate Fig. 2.

where fault-slip is oblique to these directions. The summed extension rate for 7 faults accommodating *c.* N-S extension along line Y-Y' is 0.20 mm/yr and 0.17 mm/yr for 8 faults accommodating *c.* E-W extension along line X-X'. The lengths of the transects are similar, so the E-W extension rates are of a similar order of magnitude to the N-S extension rates. If longer E-W transects were taken, crossing other N-S dip-slip faults (Fig. 1), the summed rate

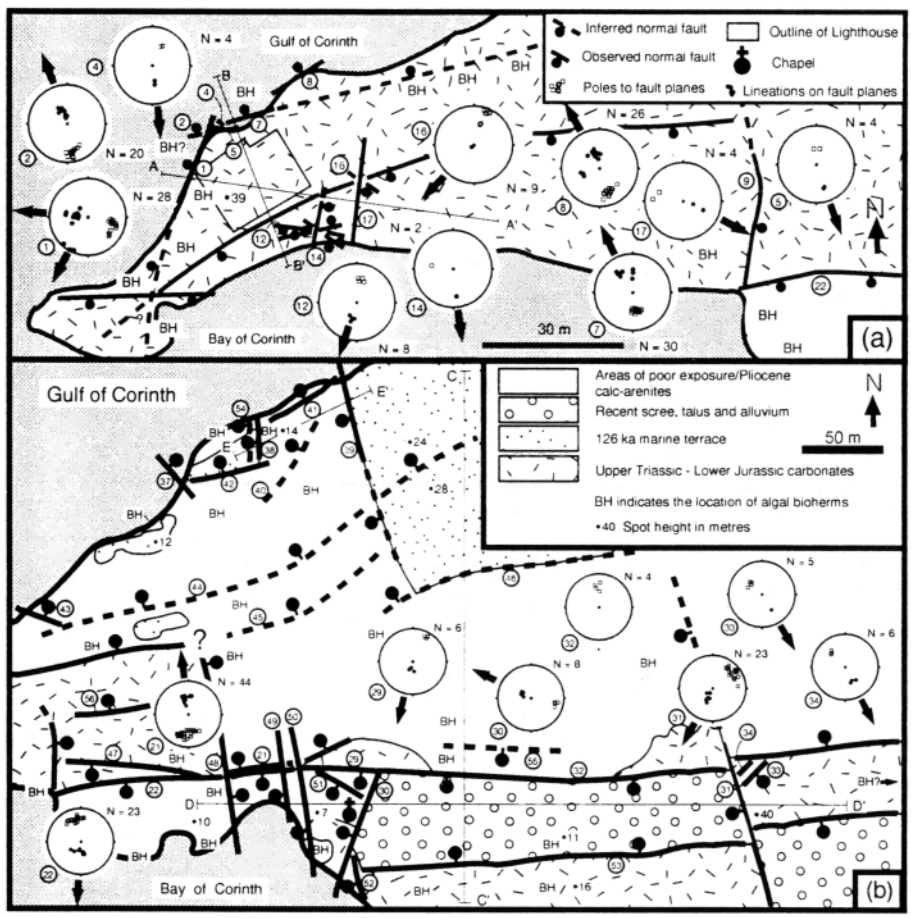

Figure 2. Fault maps of sub-areas shown in Fig. 1. Ornaments apply to both areas. Stereonets describe the fault kinematics. Heavy arrows indicate the mean fault-slip directions. Lines A-A', B-B', C-C', D-D' and E-E' locate the cross-sections in Fig. 3.

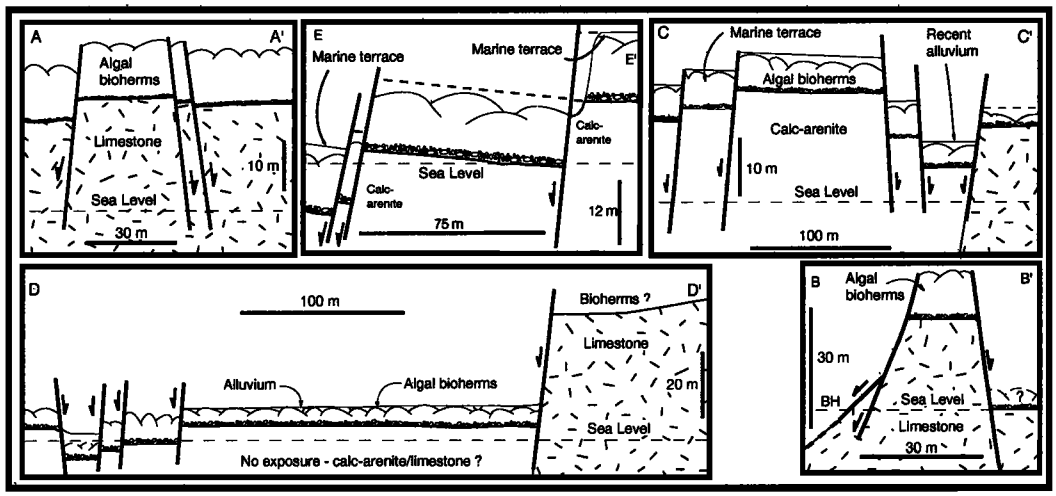

Figure 3. Cross-sections showing faulting of the uplifted 126 ka marine terrace and algal bioherms located in Fig. 2. Cobbles form the base of the algal bioherms.

Table 1. Fault orientation and deformation rate data

Fault; Mean Strike and dip; Mean plunge and direction	Throw; Displacement; Horizontal extension (m)	Average rate of throw, slip and horizontal extension over the last 126 ka (mm/yr)
1. 201/63. 60/273	4.0. 4.6. 2.3	0.03. 0.04. 0.02
2. 259/68. 67/343	20.0. 21.8. 8.5	0.16. 0.17. 0.07
4. 116/46. 37/171	?	
5. 095/36. 34/161	?	
6. ???/80. 74/326	10.0. 10.4. 2.9	0.08. 0.08. 0.02
7. 259/43. 42/343	10.0. 15.0. 11.1	0.08. 0.12. 0.09
8. 247/57. 61/326	7.0. 8.0. 3.9	0.06. 0.06. 0.03
9. 302/78.	?	
11. 117/39.	?	
12. 092/76. 70/197	?	
14. 008/46. 28/173	1.0. 2.1. 1.9	0.01. 0.02. 0.02
15. 076/56.	?	
16. 110/73. 83/219	?	
17. 013/62. 55/112	1.0. 1.2. 0.7	0.01. 0.01. 0.01
18. 104/76. *63*	10.0. 11.2. 5.1	0.08. 0.09. 0.04
19. 109/82. 82/209	?	
20. 262/53. 51/351	?	
21. 278/55. 49/348	?	
22/29. 097/64. 63/190	11.0. 12.4. 5.6	0.09. 0.10. 0.04
30. 191/66. 61/326	5.0. 5.7. 2.8	0.04. 0.05. 0.02
31. 140/68. 64/206	35.0. 38.9. 17.1	0.28. 0.31. 0.14
32. 086/53. *63*	6.0. 6.7. 3.1	0.05. 0.05. 0.02
33. 042/40. 44/149	?	
34. 047/51. 50/152	?	
35. *70. 63*	19.0. 21.3. 9.7	0.15. 0.17. 0.08
37. *66. 55/116*	11.0. 13.4. 7.7	0.09. 0.12. 0.07
38. *66. 61/326*	10.0. 11.0. 4.5	0.08. 0.09. 0.04
39. *66. 61/326*	12.8. 14.0. 5.7	0.10. 0.10. 0.05
40. *67. 49/345*	2.0. 2.7. 1.8	0.02. 0.02. 0.02
41. *67. 49/345*	5.0. 6.6. 4.3	0.04. 0.05. 0.03
42. *67. 49/345*	5.0. 6.6. 4.3	0.04. 0.05. 0.03
43. *67. 49/116*	?	
44. *67. 49/345*	4.0. 5.3. 3.5	0.04. 0.04. 0.03
45. *67. 49/345*	4.0. 5.3. 3.5	0.04. 0.04. 0.03
46. *67. 49/345*	5.0. 6.6. 4.3	0.04. 0.05. 0.03
47. *64. 63/190*	?	
48. *66. 55/116*	11.0. 13.4. 7.7	0.09. 0.12. 0.07
49. *66. 61/326*	2.0. 2.3. 1.1	0.02. 0.02. 0.01
50. *66. 61/326*	2.0. 2.3. 1.1	0.02. 0.02. 0.01
51. *64. 63/190*	?	
52. *66. 66/206*	?	
53. *67. 49/345*	5.0. 6.6. 4.3	0.04. 0.05. 0.03
54. *67. 61/326*	2.0. 2.3. 1.1	0.02. 0.02. 0.01
55. *53. 63*	6.0. 6.7. 3.1	0.05. 0.05. 0.02

Deformation rates are stated for the vertical plane containing the slip-vector azimuth. Numbers in italics are data inferred from nearby, similar faults; dip values only.

of E-W extension would increase; our value is therefore only a minimum for the entire PFSB. The overall deformation is distributed oblate vertical flattening.

Discussion and conclusions

We have shown that along-strike extension occurs between the ends of neighbouring normal fault segments, and is synchronous with fault-normal extension. The above is due to subsidence of neighbouring hangingwall basins. Along-strike extension is consistent with what we expect

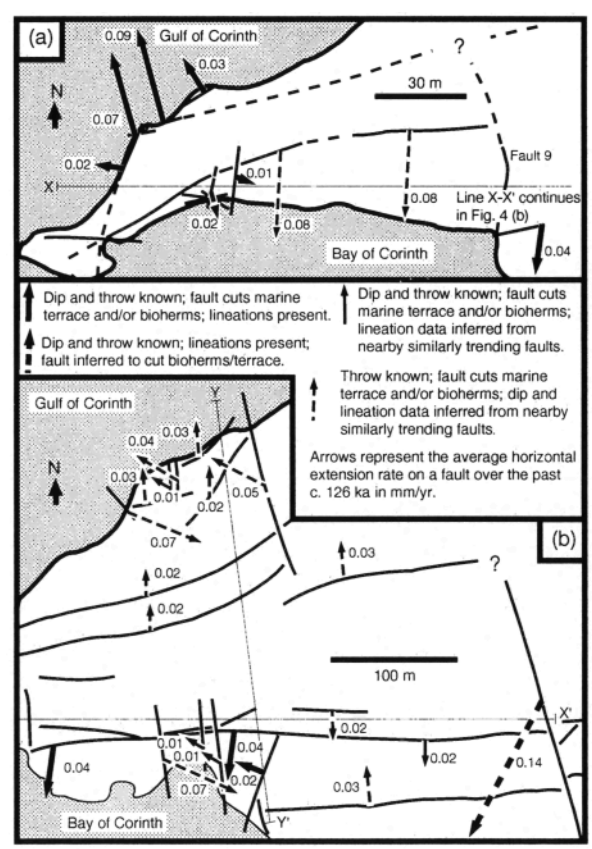

Figure 4. Horizontal velocity vector arrows for faults shown in Fig. 2. Lines X-X' and Y-Y' indicate transects along which horizontal velocities have been summed (see text for discussion).

following examination of (1) slip-directions on neighbouring faults (Fig. 1), and (2) rates from modelled and geodetically-measured earthquake motions, which show, for single points at the ends of ruptures, along-strike motions which are *c.* 20 % and *c.* 8-14 % respectively of the value for coseismic fault-slip at the centres of the ruptures (Ma & Kusznir 1995; Clarke *et al.* 1997).

The measured oblate strain within the PFSB may be linked to the observation that the 1981 rupture terminated in the vicinity: perhaps such strain is associated with increased fault strength. Similar strains may be present in the western segment boundary to the XFS which was suggested, following the 1992 Galaxidi earthquake (Ms 5.9), and its exceptional lack of aftershocks, to be a high-strength asperity along the Gulf of Corinth fault system (Hatzfield *et al.* 1996).

The horizontal velocity field in the PFSB includes components of E-W and N-S motion. In contrast, Roberts (1996) shows that along-strike motion is negligible at the centres of fault segments (Fig. 1). Such variation between oblate and plane strain within a normal fault system should be considered when trying to constrain the regional horizontal velocity field. A further complication is that, at the centres of fault segments in the Gulf of Corinth, and probably elsewhere, fault-slip rates derived directly from study of slip on faults (c. 1 mm/yr: see Pantosti *et al.* 1996) are much lower than those that include regional warping of the rocks around the faults (7-8 mm/yr: Armijo *et al.* 1996); the latter values are closer to those measured geodetically for the region (Billiris *et al.* 1991). Thus, due to distributed deformation, values for the regional extension rate should be extracted from long (tens of km) geodetic baselines across the centres of faults in order to maximise the chance of measuring the maximum value of fault-normal strain rate, and minimise the effect of along-strike motion.

Acknowledgements. This study was funded by NERC GR9/1034 and Birkbeck College (GPR), and a Birkbeck College Research Studentship (NCM). IGME and the Greig Fester Hazards Centre are thanked for support. M. Beling and A. Reynolds are thanked for field-assistance. Rachel Abercrombie and an anonymous referee are thanked for their constructive comments.

References

Abercrombie, R., I.G. Main, A. Douglas, and P.W. Burton, The nucleation and rupture process of the 1981 Gulf of Corinth earthquakes from deconvolved broad-band data, *Geophys. J. Int.*, *120*, 393-405, 1995.

Armijo, R., B. Meyer, G.C.P. King, A. Rigo and D. Papanastassiou, Quaternary evolution of the Corinth Rift and its implications for the Late Cenozoic evolution of the Aegean, *Geophys. J. Int.*, *126*, 11-53, 1996.

Billiris, H., D. Paradissis, G. Veis, P. England, W. Featherstone, B. Parsons, P. Cross, P. Rands, M. Rayson, P. Sellers, V. Ashkenazi, M. Davison, J. Jackson and N. Ambraseys, Geodetic determination of tectonic deformation in central Greece from 1900 to 1988, *Nature, 350*, 124-129, 1991.

Clarke, P.J., D., Paradissis, P. Briole, P.C. England, B.E. Parsons, H. Billiris, G. Veis and J.-C. Ruegg, Geodetic investigation of the 13 May 1995 Kozani-Grevena (Greece) earthquake, *Geophys. Res. Lett.*, *24*, 707-710, 1997.

Hatzfield, D., D. Kementzetzidou, V. Karakostas, M. Ziazia, S. Nothard, D. Diagourtas, A. Deschamps, G. Karakaisis, P. Papadimitriou, M. Scordilis, R. Smith, N. Voulgaris, S. Kiratzi, K. Makropoulos, M.P. Bouin and P. Bernard, The Galaxidi Earthquake of 18 November 1992: A Possible Asperity within the Normal Fault System of the Gulf of Corinth (Greece), *Bull. seism. Soc. Am.*, *86*, 1987-1991, 1996.

Hubert, A., G. King, R. Armijo, B. Meyer and D. Papanastassiou, Fault re-activation, stress interaction and rupture propagation of the 1981 Corinth earthquake sequence, *Earth Planet. Sci. Lett.*, *142*, 573-585, 1996.

Jackson, J.A., J. Gagnepain, G. Houseman, G.C.P. King, P. Papadimitriou, C. Soufleris and J. Virieux, Seismicity, normal faulting, and the geomorphological development of the Gulf of Corinth (Greece): The Corinth earthquakes of February and March 1981, *Earth Planet. Sci. Lett.*, *57*, 377-397, 1982.

Janecke, S.U., Structures in Segment Boundary Zones of the Lost river and Lemhi Faults, East Central Idaho, *J. Geophys. Res.*, *98*, 16223-16238, 1993.

Ma, X.Q. and N.J. Kusznir, Coseismic and postseismic subsurface displacements and strains for a dip-slip normal fault in a three-layer elastic gravitational medium, *J. Geophys. Res.*, *100*, 12813-12828, 1995.

Pantosti, D., R. Collier, G. D'Addezio, E. Masana and D. Sakellariou, Direct geological evidence for prior earthquakes on the 1981 Corinth fault (central Greece), *Geophys. Res. Lett.*, *23*, 3795-3798, 1996.

Susong, D.D., S.U. Janecke and R.L. Bruhn, Structure of a fault segment boundary in the Lost River Fault Zone, Idaho, and possible effect on the 1983 Borah Peak earthquake rupture, *Bull. seism. Soc. Am.*, *80*, 57-68, 1990.

Roberts, G.P., Variation in fault-slip directions along active and segmented normal fault systems, *J. Struc. Geol.*, *18*, 835-845, 1996.

Vita-Finzi, C., Evaluating late Quaternary uplift in Greece and Cyprus, in *Magmatic Processes and Plate Tectonics*, edited by H.M. Prichard, T. Alabaster, N.B.W. Harris and C.R. Neary, *Spec. Publ. Geol. Soc., London, 76*, 417-424, 1993.

N.C. Morewood, G.P. Roberts, The Research School of Geological and Geophysical Sciences, Birkbeck College and University College London, Gower Street, London, WC1E 6BT, U.K. (e-mail: n.morewood@ucl.ac.uk; gerald.roberts@ucl.ac.uk)

(Received May 8, 1997; Revised September 10, 1997; Accepted October 13, 1997.)